Neural Comput & Applic
DOI 10.1007/s00521-012-1255-0

ORIGINAL ARTICLE

Self-organizing map approach for classification of mechanical and rotor faults on induction motors

José M. Bossio · Cristian H. De Angelo · Guillermo R. Bossio

Received: 15 August 2011 / Accepted: 24 October 2012

Abstract Two neural network-based schemes for fault diagnosis and identification on induction motors are presented in this paper. Fault identification is performed using self-organizing maps neural networks. The first scheme uses the information of the motor phase current for feeding the network, in order to perform the diagnosis of load unbalance and shaft misalignment faults. The network is trained using data generated through the simulation of a motor-load system model, which allows including the effects of load unbalance and shaft misalignment. The second scheme is based on the motor's active and reactive instantaneous powers, in order to detect and diagnose faults whose characteristic frequencies are very close each other, such as broken rotor bars and oscillating loads. This network is trained using data obtained through the experimental measurements. Additional experimental data are later applied to both networks in order to validate the proposal. It is demonstrated that the proposed strategies are able to correctly identify, both unbalanced and misaligned load, as well as broken bars and low-frequency oscillating loads, thus avoiding the need for an expert to perform the task.

Keywords Fault diagnosis · Self-organizing maps · Neural networks · Induction motors

J. M. Bossio (✉) · C. H. De Angelo · G. R. Bossio
Grupo de Electrónica Aplicada, Fac. de Ingeniería,
Universidad Nacional de Río Cuarto,
Ruta Nac. #36, km 601, X5804BYA Río Cuarto,
Córdoba, Argentina
e-mail: jbossio@ing.unrc.edu.ar

G. R. Bossio
e-mail: gbossio@ing.unrc.edu.ar

1 Introduction

Predictive maintenance attempts to avoid unexpected faults in the industry, which cause great economic losses due to interruptions in continuous production processes. Hence, it arises the need and interest for the industry to develop strategies for on-line detection and diagnosis of incipient faults in electrical machines. In this way, process interruptions can be planned, and machines maintenance can be performed during programmed stops. This allows reducing the maintenance time and the associated economic losses.

Among various strategies actually used in predictive maintenance, those based on measurement of motor voltages and currents allow detecting different types of faults by measuring from the switchboard, thus reducing the risks for the operator in hazardous environments or difficult to access. Such strategies have also been used for detecting problems associated with the load driven by the motor.

The detection and diagnosis of electrical or mechanical faults on induction motor (IM) implies, in most cases, the interpretation of the frequency spectrum of the motor current, power, Park's vector, among others [1]. This requires an expert who performs the task, based on the information obtained from the processed signals.

At present, the study of different alternatives, such as artificial intelligence (AI) techniques, has taken great importance because they require a minimal interpretation of the studied system, that is, a detailed analysis of the mechanism or the system model is not necessary to use these techniques. Thus, the diagnosis task is simplified [2–5].

A general review of the advances on the field of electric machines and drives diagnosis based on AI, such as expert systems, fuzzy logic, neural networks among others can be found in [2].

Published online: 23 November 2012

Unsupervised neural network (UNN) was one of the AI techniques proposed for fault diagnosis on electric drives [3]. In the same work, the advantages of using UNN (in particular self-organizing maps—SOM) over perceptron type neural networks for IM condition monitoring are presented. In [4] SOM networks are used to detect and diagnose motor faults adaptively, with emphasis on faults occurred in the motors bearings. In [5] an UNN was proposed for discriminating and classifying load anomalies based on the analysis of the stator current spectrum of IM.

Usually, AI-based techniques perform the fault diagnosis from symptoms generated through a pre-processing of the input data. In electric machines, such data preprocessing is often done from the measurement of voltages and currents, and using techniques such as motor current signature analysis, active power, among others [6–8]. In [6] a method for diagnosing unbalances caused by mechanical failures in machines driven by IM and shaft misalignment between motor load using SOM networks was presented. In order to detect and classify broken rotor bars and misalignment mechanical faults that often occur in IM, a SOM-based technique is proposed in [7]. In [8] the SOM network has been successively applied for rolling bearing failures and supply asymmetry recognition, as well as early detection of stator inter-turn short circuits.

Even when other neural networks topologies have been applied for fault detection on MI, these previous works have greatly demonstrated the usefulness of SOM networks for fault classification, allowing a more general and flexible analysis of the faults [9, 10].

However, when the characteristics of the faults are very similar, or even the same, the use of only the information of the phase-current spectrum components is not enough. This is the case of broken rotor bar faults and low-frequency load oscillation. In order to improve the diagnosis, in this paper, we propose a redesign of the network, using a preprocessing of input data, from a previous result of the authors presented in [11]. Consequently, the novelty of this proposal is a new strategy for fault diagnosis that efficiently combines the SOM network design with pre-processing of input data based on the theory of instantaneous active and reactive powers. This allows obtaining an automatic diagnosis of these types of faults, which have similar symptoms and are difficult to identify, and has not been reported previously.

This second network is trained using experimental data and allows detecting and diagnosing broken rotor bars and low-frequency load oscillations. These networks may be later used to obtain an automatic diagnosis of such problems, from data obtained from measurements made in industries.

2 Self-organizing maps

Kohonen's self-organizing maps are a type of neural networks which meant to mimic in a simplified way the brain's ability to form topological maps from signals received from outside [12]. SOM-type networks are based on a competitive unsupervised learning. Because there is no output target toward which the neural network to be built, there is no external master who indicates whether the network is operating correctly or incorrectly.

The modus operandi of a self-organizing network is through the discovery of common features, correlations, regularities or categories in the input data and incorporates them into its internal structure of connections. For this reason is that neurons must self-organize according to the stimuli (data) from outside.

In competitive learning, neurons compete with each other to perform a given task, ensuring that when presented an input pattern to the network, only one output neuron (or group of neighbors) is activated. Thus, neurons compete for activation, eventually leaving only one as the winner neuron and the other forced to their minimum response values. This is with the aim of categorizing the data entering the network. For correct classification, similar values in a given category should activate the same output neuron. In addition, classes or categories must be created by the network itself, using the correlations between the input data, which is the goal of unsupervised learning.

2.1 SOM architecture

A SOM model is composed by two layers of neurons. One of them, called input layer (composed by N neurons, one for each input variable), is responsible for receiving and transmitting information from outside to the output layer. The output layer (formed by M neurons) is in charge of information processing and the construction of map features [12].

Usually, neurons in the output layer are organized in two-dimensional map, as shown in Fig. 1.

The form of connection between the two layers that compose the network is always moving forward, that is, information is propagated from the input layer to the output

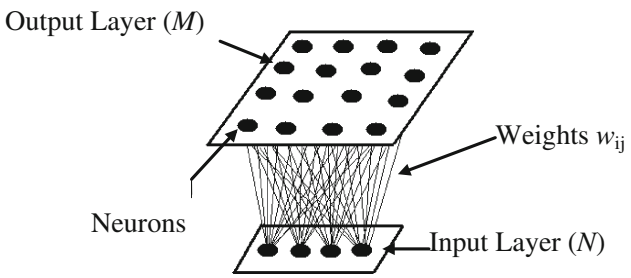

Fig. 1 SOM Architecture

layer, so that each input neuron i is connected to each output neuron j through a weight w_{ij}. Thus, the output neurons have an associated weight vector called reference vector (or codebook), as it is the prototype vector (or average) category represented by the output neuron j. Thus, the SOM defines a projection from an area of high-dimensional data in a two-dimensional map of neurons.

It should be noted that among the neurons in the output layer, there is the possibility of lateral connections of excitation and inhibition implied, without being necessarily linked, each neuron having a certain influence on its neighboring neurons. This is achieved through a process of competition between neurons and the application of a so-called neighborhood function, which produces the topology or structure of the map.

Adjacent neurons belong to a neighborhood N_j of the neuron j. The topology and the number of neurons remain fixed from the beginning. The number of neurons determines the smoothness of the projection, influencing the adjustment capacity and generalization of SOM.

In the training stage, the SOM forms an "elastic net" that folds into the original data cloud. The algorithm controls the network in a manner which tends to approximate the data density. The codebook reference vectors are close to areas where the data density is high. Occasionally few codebook vectors are in areas with low density of data.

2.2 SOM algorithm

The SOM learning process is carried out through the following two steps [13]:

First: a vector x is randomly selected from the dataset, and its distance (similarity) to the codebook vectors is calculated using Euclidean distance:

$$\|x - w_c\| = \min_j \{\|x - w_j\|\} \tag{1}$$

where c is the neuron whose weight is closest to the input vector.

Second: After finding the closest vector (or Best Matching Unit, BMU), the remainder of the codebook vectors is updated. The BMU and its neighbors (adjacent) move close to the vector x in the data space. The magnitude of the attraction is governed by the rate of learning.

As the update process occurs and new vectors are assigned to the map, the learning rate gradually decreases to zero as the radius of neighborhood.

For the update of a given reference vector, i, the following rule is used:

$$w_j(t+1) = \begin{cases} w_j(t) + \alpha(t)(x(t) - w_j(t)) & j \in N_c(t) \\ w_j(t) & j \notin N_c(t) \end{cases} \tag{2}$$

Both steps are repeated until the end of training, taking into account the number of training steps should be fixed a priori and can thus calculate the rate of convergence of the neighborhood function and the learning rate α.

Finally, after completing the training, the map is ordered in topological sense. That is, topologically closest n vectors are applied to n adjacent neurons or even within the same neuron.

2.3 SOM visualization

The most popular method to display the SOM is using unified distance matrix, **U**, which represents the map as a regular grid of neurons (each element corresponds to a neuron). When generating the matrix **U**, a matrix of distances between reference vectors of neurons contiguous in the two-dimensional map is calculated. Then, a type of graphic representation is chosen, using colors or shades of gray, so that the colors (or tones) are selected so that the shorter the distance between two neurons as darker the color between them.

3 Proposed diagnostic strategy

The objective of automatic fault diagnosis is to detect and diagnose different type of faults without the need of an expert operator. In the case of electric motor drives, it is of particular importance the precise identification of the fault origin, that is if the fault is originated in the motor itself or if the problem comes from the driven load.

Different types of faults produce, in general, different characteristic components in the frequency spectrum of the motor currents and other electrical variables. Those components are usually employed to detect and identify the drive faults.

In some cases, the characteristic fault frequencies are separated in the frequency spectrum making the design of the diagnostic strategy simpler, without the need of a great data pre-processing. This can be the case of mechanical load unbalances and motor-load shaft misalignment, principally when reduction stage exists between the motor and the load. In such case, data obtained from one motor phase current can be used to perform the diagnosis. However, when the characteristic frequencies are very close, or even the same, the use of only the phase-current spectrum components is not enough. This is the case of broken rotor bar faults and low-frequency load oscillations [11, 14, 15].

Thus, for the first case, a diagnosis strategy using SOM can be designed using only the measurement of one of the motor's phase current [6]. This network is called Network 1, and it was built and trained using data generated by simulation models which allow the drive to include the effects of mechanical unbalance and shaft misalignment. The use of a drive model allows obtaining a great amount of data from

different operating conditions (load levels and misalignment degrees), which can be difficult to obtain using experimental data. This allows improving the network training. Subsequently, experimental data obtained from measurements which correspond to a motor operating under normal conditions, unbalanced load, and motor-load coupling angular misalignment, were introduced in order to assess the ability of designed SOM network to categorize actual data.

However, as demonstrated in [11] and [16], for a correct diagnosis of broken rotor bars and low-frequency load oscillation, frequency components of the instantaneous active and reactive powers must be used. These ideas are used here to build the second network (Network 2), which is able to correctly identify between broken rotor bars and load oscillations. In this case, experimental data obtained from measurements performed in the laboratory were used to build and train the network. Measurements correspond to the cases of broken rotor bars, low-frequency load oscillation, and healthy motor, under different operation conditions. Validation was later done using new experimental data, which correspond to fault severity and operation conditions different to the used in the training stage.

4 Input data generation

4.1 Training data

Network 1: For training Network 1, input data were generated by simulation using two models. In both models, the IM was implemented in q–d variables [17], from which phase currents were obtained.

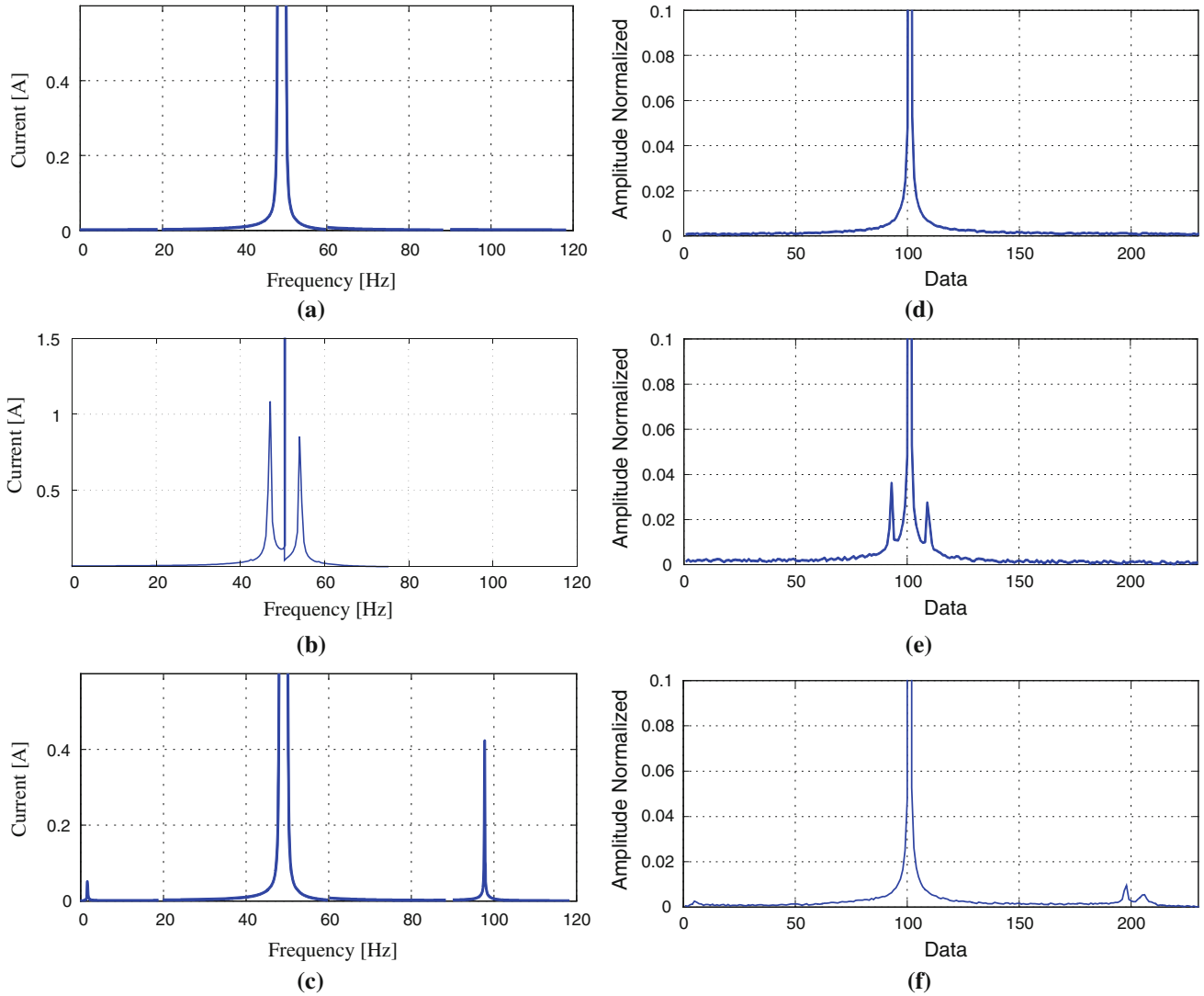

Fig. 2 Stator current spectrum obtained from simulation of a motor: **a** under normal conditions, **b** with unbalanced load, and **c** motor-load misalignment. Data used for training the network: **d** motor without mechanical unbalanced and aligned, **e** motor driving an unbalanced load, and **f** misalignment between motor and load shafts

The misalignment system (motor load) was simulated as shown in [18]. This model allows identifying the sidebands at twice the rotor frequency ($f \pm 2f_r$), characteristics of misalignment phenomena. It must be noted that, besides such components, misalignment affects the dynamic behavior of the motor, and in consequence an increase in the amplitude of the components which are associated to the static and dynamic air gap eccentricity. As for the dynamic air gap eccentricity as for the mechanical rotor unbalance and misalignment, they both produce components in the current spectrum at frequencies given by $f \pm nf_r$, which makes it possible to detect these phenomena. A further analysis on angular misalignment allows identifying not only the increase of the components at frequencies $f \pm 2f_r$, but also the sidebands at $f \pm f_r$, produced by mixed eccentricity.

On the other hand, the motor driving an unbalanced load was simulated as shown in [11]. This causes the appearance of a torque pulsation at a given frequency (f_{nd}), which is reflected in the electric motor through the speed oscillations. The speed oscillations modulate the stator currents, so sidebands around the fundamental frequency at $f \pm f_{nd}$ appear in the current spectra.

Simulation results for the motor operating under normal conditions can be seen in Fig. 2a, while those corresponding to load unbalance and motor-load misalignment in Fig. 2b, c, respectively. In the case of misalignment, a variation of angle between 0° and 5° was first evaluated, with an 80 % load in all cases. Finally, a 2° misalignment case was used because it corresponds to the most significant magnitude that can be found in industry applications, and it does not produce a significant reduction in the lifetime of couplings o other components. For the case of load unbalance, a slope (inclination) in the plansifter of 1° with respect to the horizontal was considered, which is similar to the inclination found in the industry case. In these

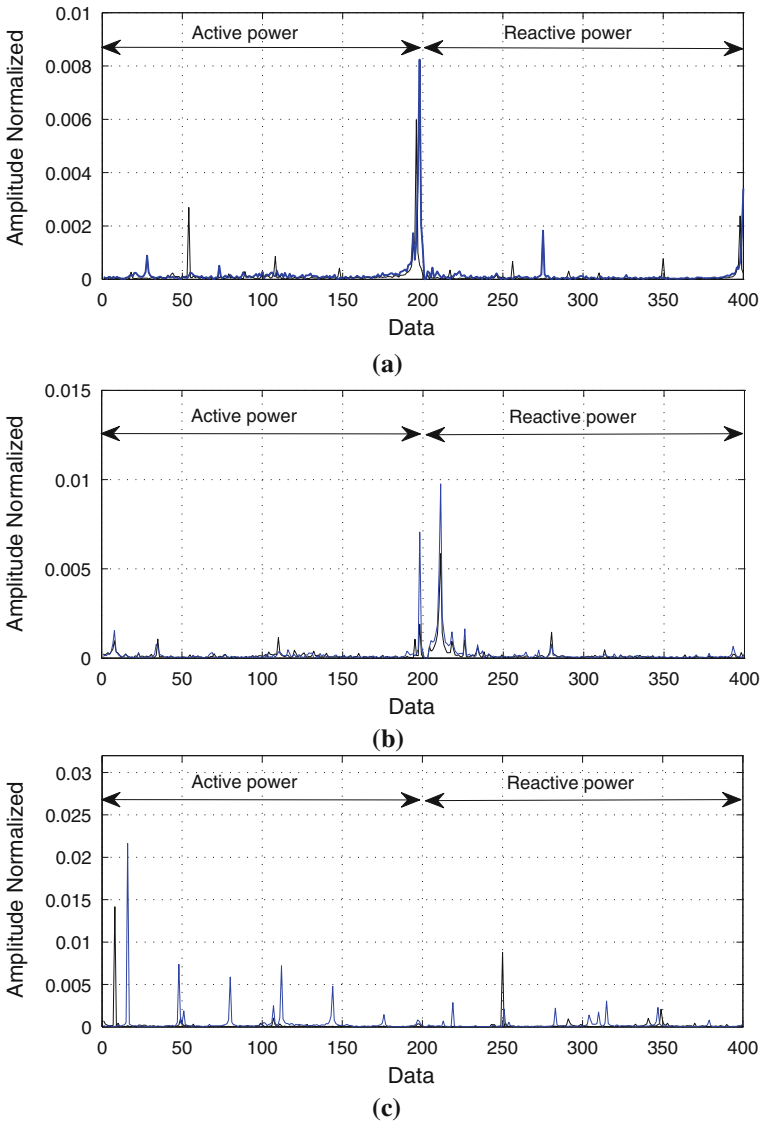

Fig. 3 Data use for training the network (spectrum of instantaneous active and reactive powers): **a** healthy motor, **b** broken bars **c** with load fluctuations

figures, the frequency components in stator current spectra for the analyzed faults can be clearly identified.

To create the input data used for training the network, a selection of 250 points in the stator current spectrum between 0 and 120 Hz, obtained by simulation, were initially used. These data were normalized in order to make them independent of the load level. The normalization of data was performed by dividing the elements of the input vector, corresponding to the stator current spectrum, by the largest element of such vector.

Thus, it was possible to visualize both sidebands produced by the load unbalance, as those caused by shaft misalignment. Then, noise was introduced in the normalized interval, so as to produce a scatter in network training data. Figure 2 shows the final data used for training the network, corresponding to the three cases: the motor in normal conditions (d), the motor driving an unbalanced load, where the characteristic frequencies are close to data 90 and 110 (e), and misalignment between the motor and the load shafts (f), where the characteristic frequencies are close to data 1 and data 200.

Network 2: In the second case, input data were generated by experimentally measured data, with the aim of getting closer to the actual application case. Besides the difference between the types of faults, the data include variation in the magnitude of the fault and in the percentage of motor load.

The asymmetry due to broken rotor bars is reflected in two components in the current spectrum, particularly in the frequencies $f \pm 2sf$. The magnitude of these sidebands depends on the load and inertia of the motor-load system, as well as the severity of the fault [19, 20]. In addition, these sidebands may even appear in a healthy motor, when the driven load is pulsating and/or oscillating, that is when the load torque varies with the position of the motor [21].

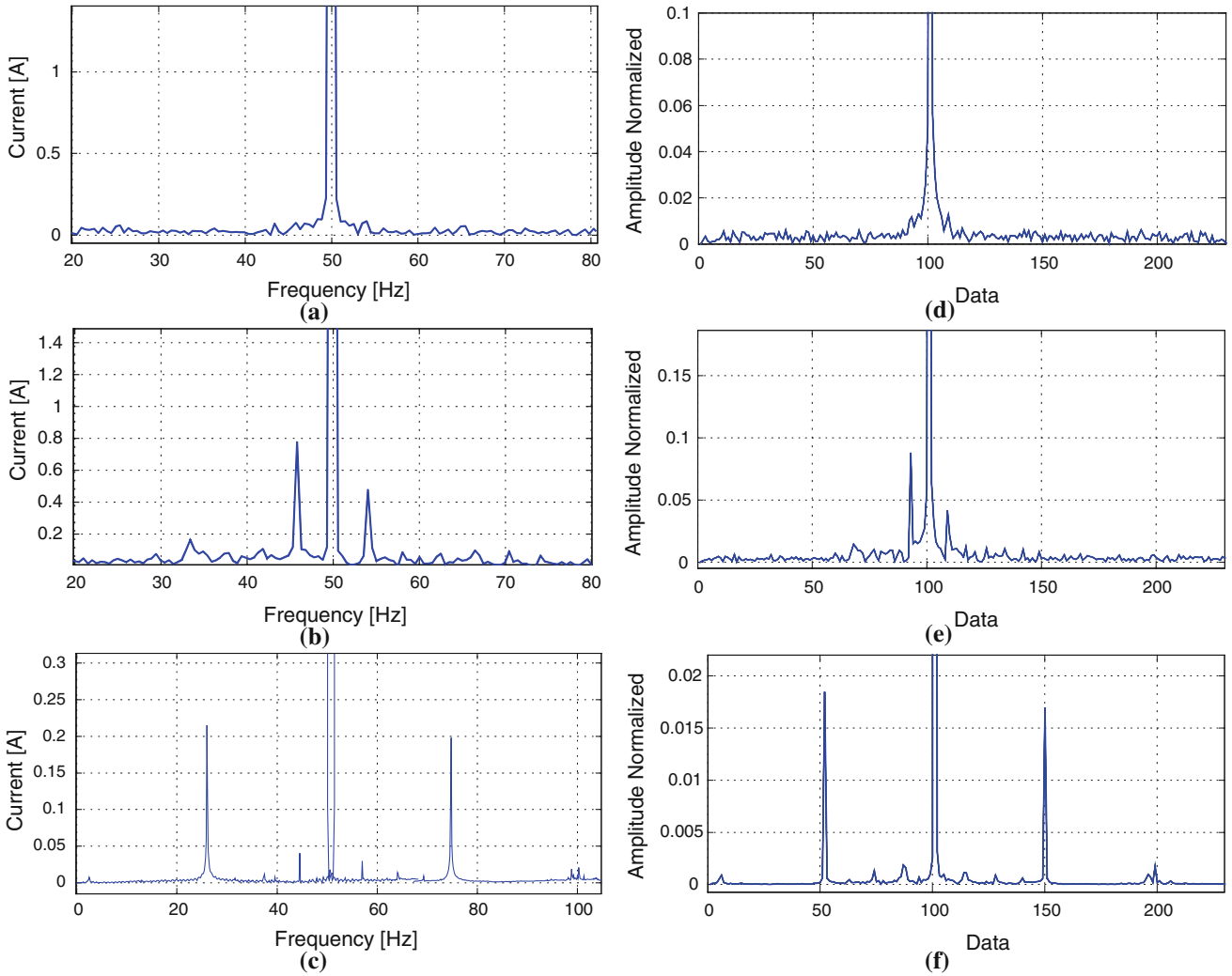

Fig. 4 Stator current spectrum obtained from measurement on a motor: **a** under normal conditions, **b** motor driving an unbalanced load, and **c** misalignment between motor and load shafts. Data for validating the network: **d** motor under normal conditions, **e** motor driving an unbalanced load, and **f** misalignment between motor and load shafts

Because of this, the data entered into the network are obtained by a frequency analysis of the instantaneous active and reactive power of the motor [11, 16]. This allows to correctly separating both types of faults, by the characteristic frequencies in the low-frequency range of the instantaneous powers spectra. Broken rotor bars fault mainly appears as low-frequency components at $2sf$ in the instantaneous reactive power spectrum, but not in the instantaneous active power spectrum. On the contrary, load oscillation produces characteristics frequency components of higher amplitude in the active power spectrum, while they are practically negligible in the reactive power spectrum.

To create the input data used in training Network 2, we proceeded to form a set of 400 points concatenated: the first 200 correspond to the instantaneous active power spectrum and the remaining 200 to the instantaneous reactive power spectrum. Thus it was possible to visualize the range of characteristic frequencies present in the active and reactive powers respectively, produced by the broken bars, as well as those caused by load fluctuations at low frequencies. With this particular construction of the input data set, we are able to feed the network with patterns which are different enough for each type of fault.

Figure 3 shows the data used for training the network. It can be observed the following cases: Fig. 3a corresponds to the healthy motor with 40 % load (blue line) and 80 % load (black line); Fig. 3b to the motor with 1 broken bar (blue line), and 2 broken bar (black line), both with 75 % load; and Fig. 3c the motor driving an oscillating load. This load is composed by a constant 75 % load torque plus a 3 % amplitude, 2 Hz square wave load torque (blue line), and a

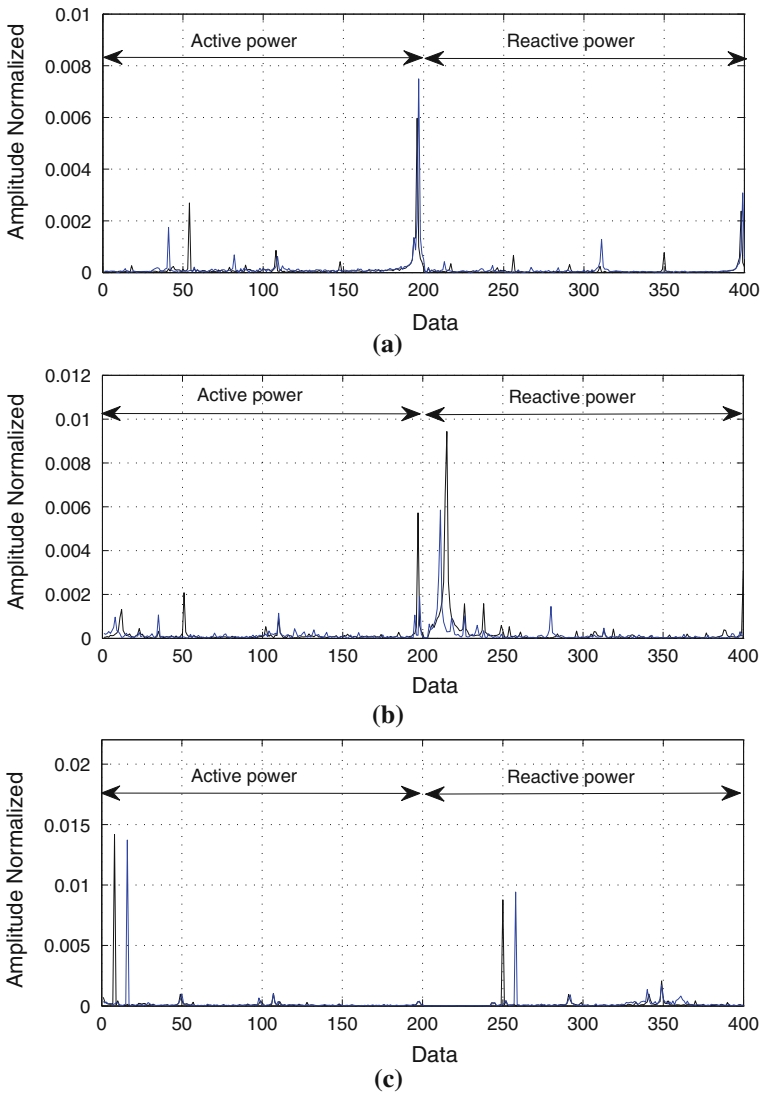

Fig. 5 Data for validating the network (*blue line*), compared with training data (*black line*): **a** healthy motor, **b** broken rotor bars **c** with load oscillations (color figure online)

3 % amplitude, 1 Hz sinusoidally oscillating load torque (black line). The criteria used in selection of data for training aimed to include greater diversification of possible cases within each set of different faults.

4.2 Validation data

Network 1: Experimental data used for validating the proposal were obtained both from drives installed in the industry and from a laboratory setup. The cases presented here correspond to measurements made on plansifters driven by IM, both in normal conditions, as in conditions of load unbalance, and measurement obtained in the laboratory for a motor-load misalignment case.

Through the analysis of experimental results, it was possible to discriminate through the stator current spectrum, the characteristic frequencies for each case of failure. The results for the motor operating under normal conditions, driving an unbalanced load, and with shaft misalignment can be seen in Fig. 4a, b, c, respectively. The misalignment case corresponds to a 2° angular misalignment, with 80 % load, while the case of load unbalance corresponds to a plansifter inclination of approximately 1° with respect to the horizontal.

For the validation of the network, the input data correspond to those obtained from the experimental tests normalized in the same way as data obtained from simulation, through a selection of 250 points of the stator current spectrum. Currents were acquired using an oscillographic register measuring 64,000 samples at a sampling frequency of 8 kHz, and in a time of 8 s. Figure 4 shows these data for the three cases of study.

It should be further noted that, besides the characteristic frequencies produced by misalignment, Fig. 4f shows some components produced by eccentricity, both in the data 50 (25 Hz), as in the data 150 (75 Hz).

Network 2: The experimental data used for validating the proposal were obtained from a laboratory setup, both for broken bars, as for load fluctuations. Data were processed the same as the training data. However, operation conditions and fault severities different from the measured in the training stage were used for validation.

Figure 5 shows the spectra of the validation cases (blue line), while the training data are also shown for comparison (black line): Fig. 5a shows data corresponding to the healthy motor, with 60 % load (validation) and 80 % load (training); Fig. 5b corresponds to the motor with 2 broken bars at 50 % load (validation), and at 75 % load (training), where it was considered 2 broken bars from a total of 40 rotor bars which has the rotor (5 %), so as not to affect the motor operation; and Fig. 5c presents data from the motor-load set with oscillating load at 2 Hz (validation), and 1 Hz (training), both sinusoidal signals.

5 Implementation and visualization

The self-organizing map network was implemented by using the SOM toolbox, from Matlab [13]. Once the input data were processed and normalized as explained in the previous section, they were placed in a special data structure used by SOM toolbox to group information about the system data in one place. The argument of such structure is the data matrix itself, which contains the name given to the

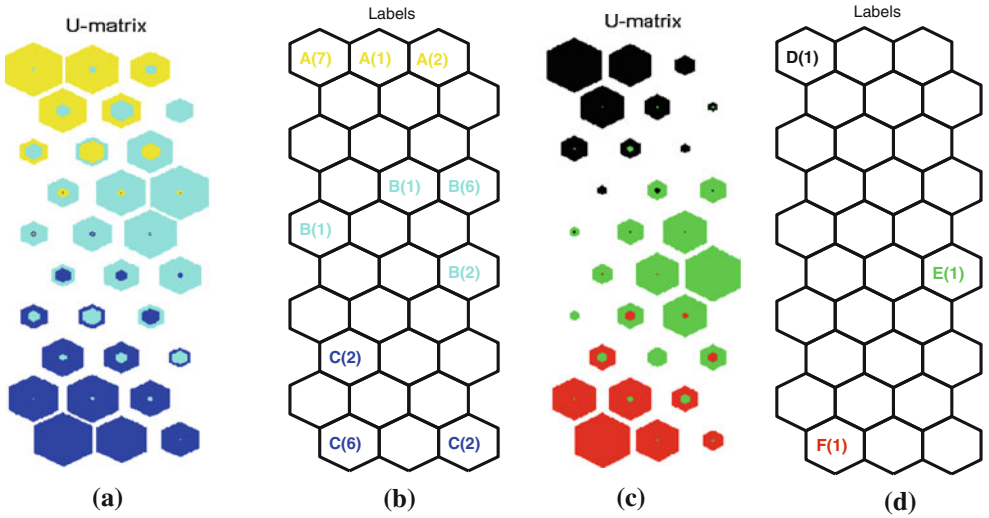

Fig. 6 Simulation data: **a** multiple histograms, **b** location tags. *A* Shaft misalignment; *B* motor operating in normal conditions; and *C* motor driving an unbalanced load. Experimental data: **c** Multiple histograms, **d** Location tags. *D* Shaft misalignment; *E* motor operating in normal conditions; and *F* motor driving an unbalanced load

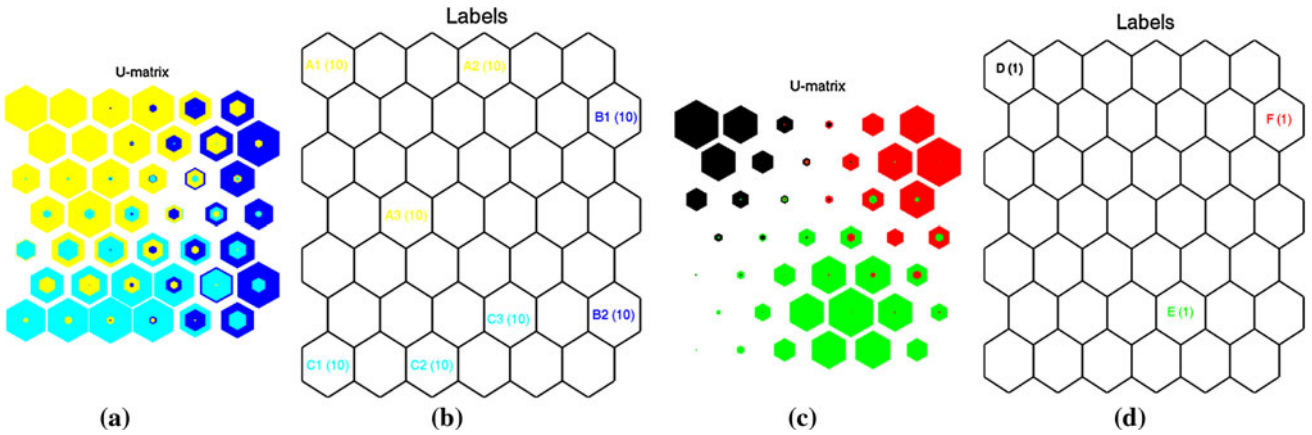

Fig. 7 Training data: **a** multiple histograms, **b** location tags, *A1*, *A2*, *A3* the motor with the broken bars, *B1*, *B2* the motor without faults, and *C1*, *C2*, *C3* the motor with pulsating load. Validation data: **a** multiple histograms, **b** location tags, *D* the motor with the broken bars, *E* the motor with pulsating load, and *F* the motor without faults

data system, and the names of the components (variables) in the matrix data.

5.1 Training of the map

The SOM_MAKE function was used to train the SOM. By default, it first determines the size of the map, then sets the map using linear initialization, and finally performs the training of the map.

Network 1: The data structure consists of 10 samples from each case (a total of 30 samples) where they represent the case of motor-load shaft misalignment, the motor without mechanical unbalance and aligned, and the motor driving an unbalanced load. Then, a label is associated with each case: A, B and C respectively.

Network 2: In the second network model, the data structure consists of 10 samples for each case (a total of 80 samples), corresponding to the motor with 1, 2 bars and 3 broken rotor bars (the three cases with 50 % load), the motor driving a sinusoidally oscillating load at 2 and 1 Hz, and a square wave load at 2 Hz, and finally to the healthy motor operating at 40 and 60 % constant load torque.

5.2 Map display

Network 1: The output layer consists of 30 neurons, which are responsible of processing and formation of the map of features. This map is organized in a two-dimensional map, using a hexagonal topology, so as to obtain a better relationship between neurons.

For visualizing the results, the matrix of unified distances (or **U** matrix) is usually used, which shows the distances between neighboring units, and thus visualizes the structure of clusters of the map (typically uniform areas of low values). Another important tool in the analysis of data using a SOM is the histograms of success. They are formed by taking a data structure, finding the BMU of each sample of the map data, and increasing a counter each time a unit of the map correspond to the BMU. So, the histogram of success shows the distribution of the data structure on the map.

In this work, multiple histograms are represented simultaneously in the **U** matrix. The map created for the studied cases, which consist of three clusters, is represented on a regular grid of 3 × 10 neurons, so that each element represents a neuron. The size of the neurons gives notion

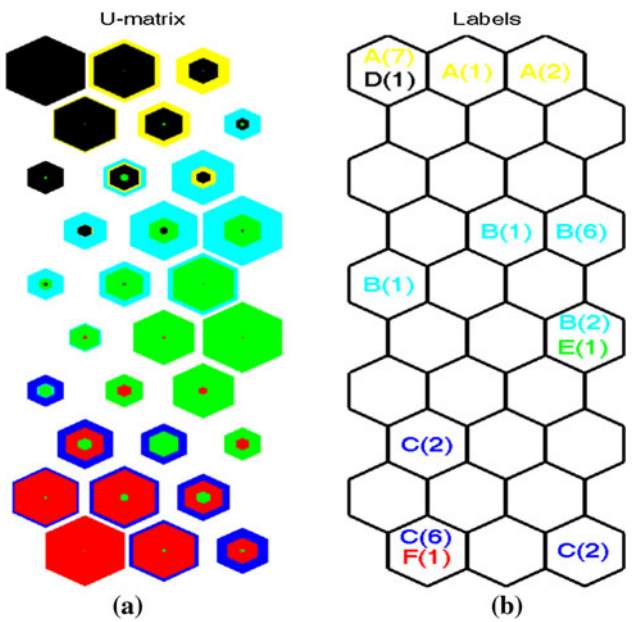

Fig. 8 Simulation and experimental data: **a** multiple histograms, **b** location tags. *A–D* Shaft misalignment; *B–E* motor operating in normal conditions; and *C–F* motor driving an unbalanced load

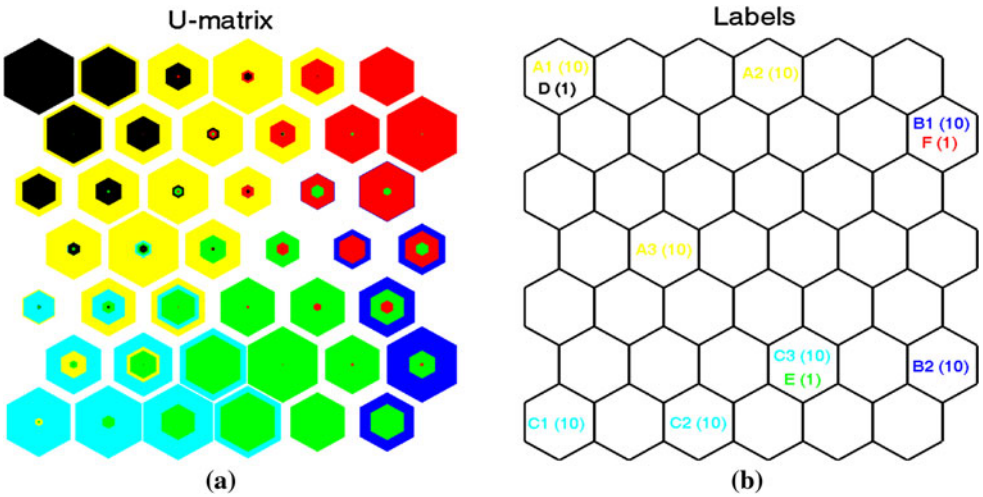

Fig. 9 Training and validation data. **a** Multiple histograms, **b** location tags. *A–D* The motor with the broken bars, *B–F* the motor without faults, and *C–E* the motor with pulsating load

about the amount of hit values and the relative goodness of each map unit in representing the data, so that the greater one of the same color set denotes the higher match with its corresponding cluster.

The mode of graphical representation of the selected map (different colors) allows differentiating the healthy case and the two cases of faults, as shown in Fig. 6a, through data obtained by simulation, and Fig. 6c by using the data obtained experimentally. In both cases, the clusters corresponding to the different cases are shown. As shown in Fig. 6b, it is possible to discriminate three different clusters, two of them due to the studied faults and one to the healthy motor. Specifically, it shows the motor without faults (cyan), the motor with load unbalance (blue) and the case of shaft misalignment (yellow). Figure 6d shows the results obtained by using experimental data. In this case, the green color corresponds to the healthy motor, the red color to the motor with mechanical load unbalance, and finally the black color to the misalignment between shafts. In these figures, the number in brackets shows the frequency of occurrence of the data used for the training and validating the network.

Network 2: The output layer is formed by 42 neurons, responsible for processing and form the map of features, organized as a two-dimensional map. The hexagonal topology is used as in the previous network.

The map created for this network model was performed in a regular grid of 7 × 6 neurons, so that each element represents a neuron. Figure 7a shows the multiple histograms for the data used for training, where it is possible to discriminate three different clusters, two of them due to faults in study, and the other to the healthy motor. Specifically, it shows the motor without faults (blue), the motor with the broken bars (yellow), and finally the pulsating load cases (cyan). Figure 7b shows the location tags, with the corresponding number of hits. Figure 7c, d shows the results obtained for the data used for validation, as well as the different labels for each case.

5.3 Analysis of results

Network 1: Finally, both the training data (simulation) and the validation data (experimental) are represented together in Fig. 8. A clear distribution of the clusters, depending on the type of fault, can be seen. Even when experimental data present some components which were not considered in the training data (e.g., the components due to eccentricity for the misalignment case), a correct fault identification is obtained for all the studied cases.

Network 2: In the analysis of the second network SOM using experimental data, we could observe a clear distribution of clusters according to the type of fault present. While the validating data show some variations such as the percentage of tested motor load, or different load oscillation, a correct identification of faults in all cases studied is obtained. This analysis is presented in Fig. 9 for the three cases considered.

6 Conclusions

In this paper, two schemes for fault diagnosis using unsupervised neural networks of the type self-organizing map were presented. The first model of the network was implemented for the diagnosis of failures caused by mechanical load imbalances on induction motors drives, and misalignment between the motor and load shafts. Since these faults produce symptoms (components in the current spectrum) which are different, a single motor phase current can be used for obtaining a correct diagnosis. However, when faults produce similar symptoms, that is having the same characteristic frequencies in the phase-current

spectrum, as the case of broken bars and low-frequency oscillating load, a different strategy must be used. For such a case, a second network was implemented based on measurements of instantaneous active and reactive power, by properly arranging the input data of the network. This allows to obtain a correct fault diagnosis and identification even for this type of faults.

For the first case, network training is performed using data obtained from the simulation of a model of MI, which can represent the behavior of the normal operating conditions, in conditions of mechanical load imbalance and shaft misalignment. Network 2 is trained by experimental data, obtained from tests on motors driving a load with low-frequency torque oscillations and a motor with different number of broken rotor bars.

Validation is performed using data different from those used for training. For the Network 1, data were obtained from measurements made on plansifters driven by induction motors, both under normal conditions and in conditions of equipment imbalance, and motors with misalignment between the motor and load shafts. For Network 2, validation was carried out by experimental data on both normal motor operating conditions, as in conditions low-frequency load oscillation and broken rotor bars, at different load levels not considered in the training stage.

The analysis of the results obtained through the implementation of both networks allowed to clearly "see" the separation, or discrimination, through three well-defined areas (clusters). The location of the labels in clusters validated the implementation of the networks.

Thus, by applying artificial neural networks (SOM), it was possible to correctly diagnose and identify different types of faults in electrical machines, with a minimum interpretation of the system under study.

References

1. Bellini A, Filippetti F, Tassoni C, Capolino GA (2008) Advances in diagnostic techniques for induction machines. IEEE Trans Ind Electron 55:4109–4126
2. Filippetti F, Franceschini G, Tassoni C, Vas P (2000) Recent developments of induction motor drives fault diagnosis using AI techniques. IEEE Trans Ind Electron 47(5):994–1004
3. Penman J, Yin CM (1994) Feasibility of using unsupervised learning, artificial neural networks for the condition monitoring of electrical machines. IEE Proc Electr Power Appl 141(6):317–322
4. Zhong F, Shi T, He T (2005) Fault diagnosis of motor bearing using self-organizing maps. Electr Mach Syst ICEMS 3:2411–2414
5. Salles G, Filippetti F, Tassoni C, Grellet G, Franceschini G (2002) Monitoring of induction motor load by neural network techniques. IEEE Trans Power Electron 15(4):762–768
6. Bossio JM, De Angelo CH, Bossio GR, García G (2010) Fault diagnosis on induction motors using self-organizing maps. In: The 9th international conference of the IEEE/IAS industry applications
7. Germen E, Gökhan ED, Gerek ÖN (2007) Self organizing map (SOM) approach for classification of mechanical faults in induction motors, In: International work-conference on artificial neural networks, LNCS 4507, Springer, pp 855–861
8. Kowalski CT, Orlowska-Kowalska T (2003) Neural networks application for induction motor faults diagnosis. Math Comput Simul 63(3–5):435–448
9. Kato T, Inoue K, Takahashi T, Kono Y (2007) Automatic fault diagnosis method of electrical machinery and apparatus by using Kohonen's self-organizing map. In: Power conversion conference, pp 1224–1229
10. Sid O, Menaa M, Hamdani S, Touhami O, Ibtiouen R (2011) Self-organizing map approach for classification of electricals rotor faults in induction motors. In: EPECS, pp 1–6
11. Bossio G, De Angelo C, Bossio JM, Pezzani C (2009), Separating broken rotor bars and load oscillations on IM fault diagnosis through the instantaneous active and reactive currents. IEEE Trans Ind Electron, 56:4571–4580. ISSN:0278-0046
12. Kohonen T (2001) Self organizing maps, 3rd edn. Springer, Berlin
13. Vesanto J, Himberg J, Alhoniemi E, Parhankangas J (2000) SOM toolbox for Matlab
14. Long W, Habetler TG, Harley RG (2005) Separating load torque oscillation and rotor fault effects in stator current-based motor condition monitoring. In: IEEE international conference on electric machines and drives, pp 1889–1894
15. Wu L, Habetler, TG, Harley RG (2007) A review of separating mechanical load effects from rotor faults detection in induction motors. In: IEEE international symposium on diagnostics for electric machines, power electronics and drives, pp 221–225
16. De Angelo C, Bossio G, Garcia G (2010) Discriminating broken rotor bar from oscillating load effects using the instantaneous active and reactive powers. Electr Power Appl 4:281–290. ISSN: 1751-8660
17. Krause PC, Wasynczuk O, Sudhoff SD (1996) Analysis of electric machinery. IEEE Press, New York, pp 133–210
18. Bossio JM, Bossio GR, De Angelo CH (2009) Angular misalignment in induction motors with flexible coupling. In: The 35th annual conference of the IEEE Industrial Electronics Society
19. Bellini A, Filippetti F, Franceschini G, Tassoni C, Kliman GB (2001) Quantitative evaluation of induction motor broken bars by means of electrical signature analysis. IEEE Trans Ind Appl 37(5):1248–1255
20. Verucchi CJ, Acosta GG, Carusso E (2005) Influence of the motor load inertia and torque in the fault diagnosis of rotors in induction machines. IEEE Lat Am Trans 3(4):48–53
21. De Angelo C, Bossio G, Bossio JM, Garcia G (2008) Broken bar detection in single-phase reciprocating compressors. In: The 34th annual conference of the IEEE Industrial Electronics Society, pp 1125–1130